Thermochimica Acta, 170 (1990) 179–188
Elsevier Science Publishers B.V., Amsterdam

INVESTIGATION OF SUBBITUMINOUS COALS BY THERMOGRAVIMETRY–MASS SPECTROMETRY. PART 2. FORMATION OF OXYGEN- AND SULPHUR-CONTAINING PRODUCTS. KINETICS OF THE OVERALL MASS LOSS

PIROSKA SZABÓ, GÁBOR VÁRHEGYI, FERENC TILL and TAMÁS SZÉKELY

Research Laboratory for Inorganic Chemistry, Hungarian Academy of Sciences, P.O. Box 132, Budapest 1502 (Hungary)

(Received 28 February 1990)

ABSTRACT

Results derived from the experiments of Part 1 of this paper (Szabó et al., Thermochimica Acta, 170 (1990) 167) are presented. The mass spectrometric intensities of the oxygen-containing decomposition products, as functions of the temperature, were wide curves with multiple peaks indicating the multiple sources of these compounds. H_2S, COS, CS_2 and CH_3SH evolved mainly in the temperature range of the decomposition of aliphatic structures. Their intensity curves, however, showed a second, sharp peak due to a reaction between iron sulphide, formed from pyrite, and water. SO_2 is believed to be a secondary product of pyrite decomposition. The kinetic evaluation of the mass loss of the sample was based on thermogravimetric results at heating rates of 5, 10, 20, 40 and 80 °C min^{-1}. Parallel reactions were assumed without any restriction on the distribution of the activation energies and pre-exponential factors. The results indicated that the unimolecular dissociation of the chemical bonds may be rate-determining factors only at higher temperatures, after the evolution of more than 60% of the volatile matter from the sample. Below this region, low activation energies and pre-exponential factors were observed which may be due to diffusion control (at low temperatures) and a radical mechanism (at medium temperatures).

INTRODUCTION

In Part 1 of this paper [1] hydrocarbon evolution from a series of coals was discussed. Two separate topics from the same study remained for the present paper: the formation of oxygen- and sulphur-containing products and the kinetics of the overall mass loss of the sample during the thermal decomposition. The oxygen and sulphur atoms play a very important role in coal processing. Their transformation during coal pyrolysis was reviewed by Attar and Hendrickson [2]. Recently Calkins [3] analysed the role of pyrite in the formation of sulphur-containing products. Levy and White [4] showed that water vapor, forming abundantly in the thermal decomposition of coal,

0040-6031/90/$03.50

catalyses pyrite decomposition. Chatterjee et al. [5] presented new, controversial data about the sources of carbon dioxide formed during coal pyrolysis. The state of the art in coal pyrolysis kinetics was extensively reviewed by Gavalas [6]. Serio et al. [7] elaborated sophisticated mathematical models based on a combination of 20 partial reactions, each of them described by a Gaussian distribution of activation energies. Burnham et al. [8] assumed a general, non-Gaussian distribution for the activation energy and approximated it by a discrete distribution function.

The aim of the present paper is to provide additional data about the formation of the heteroatom-containing products. During the kinetic evaluation of the overall mass loss of the sample we accepted that the pyrolysis can be approximated by a continuous, non-Gaussian distribution of partial reactions [8]. The assumption of a common pre-exponential factor, however, was not accepted and only simple calculations based on experiments at several heating rates were carried out.

EXPERIMENTAL

The apparatus, samples and experimental procedure were described in Part 1 of the paper [1]. For the kinetic calculations TG curves were measured at heating rates of 5, 10, 20, 40 and 80 °C min^{-1}. Sulphur analysis data of the coal samples, provided by the Central Development Institute for Mining (Budapest), are shown in Table 1.

RESULTS AND DISCUSSION

Oxygen-containing products

Water, carbon monoxide and carbon dioxide evolved in wide temperature domains (see Fig. 1). Their mass spectrometric intensity curves, as functions of temperature, were composed of overlapping peaks indicating several

TABLE 1

The sulphur content (%, dry base) of the coal samples

Sample	Ash	S_{tot}	S_{pyr}	S_{sulph}	S_{org}
M-1	44.6	2.5	1.8	0.1	0.7
M-2	49.8	3.8	2.4	0.2	1.1
S	31.7	0.3	< 0.1	< 0.1	0.2
K-1	25.4	4.1	1.7	0.3	2.1
K-2	23.3	4.7	1.0	0.4	3.3

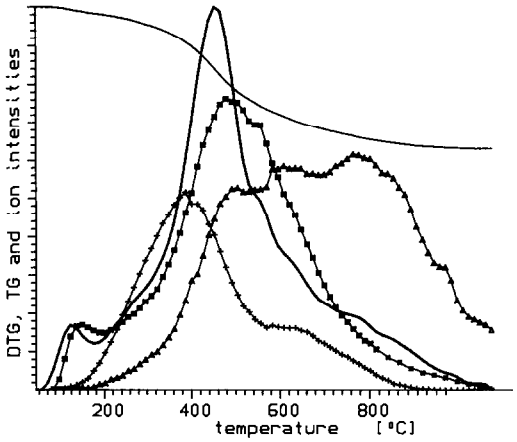

Fig. 1. TG–MS data of coal K-2: ———, TG and DTG; –■–, H_2O, –▲–, CO; – + –, CO_2.

different sources of these products. The sources of water in the order of their thermal stability are as follows: absorbed water, water molecules attached to the cations of the carboxyl groups of the coal and the various types of OH groups. According to the literature, carbonic acids and their salts and esters evolve carbon dioxide during pyrolysis whereas quinones, ethers, and ketones mainly yield carbon monoxide [2,5]. The mineral matter may also contribute to the water and carbon dioxide production. Clay minerals produce water from about 100 °C to 900 °C. At the applied experimental conditions the thermal decomposition of the iron carbonates starts at about 600 °C while the more stable $CaCO_3$ minerals decompose at about 700–800 °C. In this way the high temperature tail of the CO_2 curve shown in Fig. 1 may be due to the mineral content. In agreement with Schaffer's work [9,10] we observed a correlation between the amounts of H_2O and CO_2 formed below the region of carbonate decomposition. As Fig. 2 shows, the first peak of the carbon monoxide curve, about 500 °C, is near the peaks of the C2–C4 aliphatic products and phenols and the first peak of benzene. This observation indicates that some of the CO is probably formed from aliphatic–aliphatic ether structures in a radical decomposition mechanism. Phenols are believed to be formed mainly from aliphatic–aromatic ethers [2,11]. The next peak of CO emission, at about 600 °C, coincides with the second benzene peak, suggesting that the rupture of the aromatic–aromatic ether bridges produces CO. The maximum of the CO production, around 800 °C, agrees well with the peak of the H_2 evolution, indicating that a major portion of the CO arises from oxygen-containing heterocycles at the same time as the fusion of the lamellae produces H_2 also, during the formation of the char structure. The evolution of H_2, H_2O, CO and CO_2 is probably influenced by the well-known secondary reactions $H_2O + C \rightleftharpoons H_2 + CO$ and $2CO \rightleftharpoons CO_2 + C$.

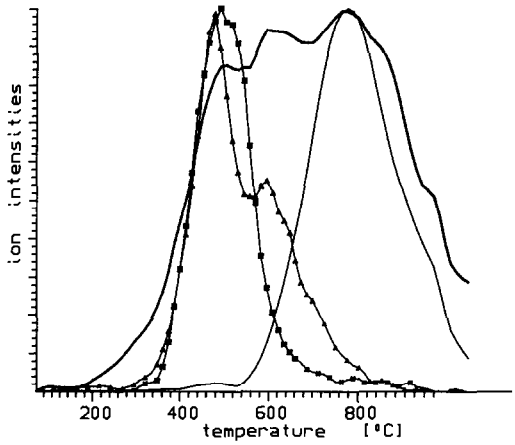

Fig. 2. Comparison of the evolution of H_2 (———, $m/z = 2$), CO (———, $m/z = 28$), benzene (-▲-, $m/z = 78$) and phenol (-■-, $m/z = 94$) from coal K-2. (The curves are magnified to equal heights for clarity).

Sulphur-containing products

The thermal decomposition of coals containing considerable amounts of sulphur produces relatively high amounts of H_2S and SO_2 and smaller amounts of CH_3SH, COS, CS_2, thiophene and various substituted thiophenes [3]. Under typical mass spectrometric conditions (electron impact ionisation with 70 eV electron energy), the production of H_2S, CH_3SH, COS and CS_2 can be measured by the intensities of mass spectrometric fragments with $m/z = 34$, 47, 60 and 76 respectively. Thiophene is a major contributor to the fragment with $m/z = 84$. In our experiments fragments with $m/z = 48$ and 64 formed almost exclusively from SO_2. (Their intensity ratio corresponded to the fragmentation of SO_2 and their intensities, as functions of temperature, fitted each other well and differed in shape from any other intensity curves.) As Fig. 3 shows, the evolutions of the various sulphur-containing products considerably differed from each other. The magnitudes of the intensities strongly depended on the organic and mineral sulphur contents of the coals. The amount of SO_2 formed, estimated by the integral of the corresponding intensities, had shown a good correlation with the pyrite content of the samples. This observation agrees with Calkins' results [3], who investigated the decomposition of a coal of high pyrite content in an inert atmosphere and showed that the mechanical removal of the mineral content reduces the amount of SO_2 formed almost to zero. He also noted that other possible sources of SO_2, such as organic sulphones, appear to be very scarce or absent in most coals. It is an open question, however, as to how the sulphur content of the pyrite (or any other sulphur-containing source structure) can obtain oxygen to form SO_2. Note that the concentration of the oxygen traces in the ambient gas was about 0.02% and a high gas flow

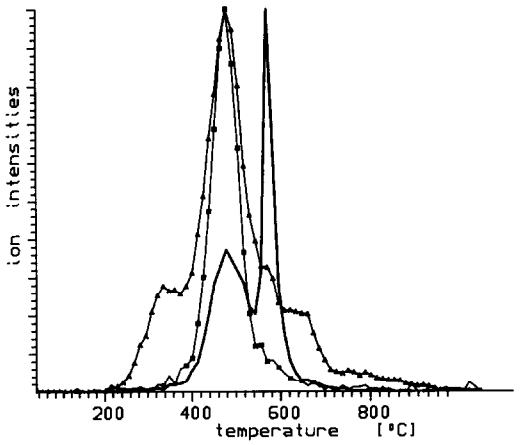

Fig. 3. Comparison of the evolution of sulphur-containing products from coal M-1: ———, H_2S ($m/z = 34$); –▲–, SO_2 ($m/z = 64$); –■–, thiophene ($m/z = 84$). (The curves are magnified to equal heights for clarity.)

rate was applied to sweep away the formed products quickly from the vicinity of the sample. The low concentration of oxygen is obviously not sufficient to oxidise the pyrite in the sample. One can imagine, however, that elemental sulphur (S_2–S_8) evolving from pyrite as well as some labile sulphur containing intermediate products can react with the oxygen traces even in the cooler part of the TG furnace and in the moderately heated capillary connecting the furnace to the ion source. The concentration of the SO_2 that formed in the ambient gas was lower than 0.01%, so the amount of oxygen was in excess for this oxidation. Similar problems may arise in other types of equipment also, explaining the high SO_2 production reported by other investigators [3]. It may be interesting to note that SO_2 formation started at about 260 °C in our case (see Fig. 3) while the usual decomposition temperature of pyrite is about 600 °C in an inert atmosphere [4]. This observation indicates some interaction between pyrite and the decomposition products of coal.

The intensity curve of hydrogen sulphide showed a characteristic, sharp second peak between 560 and 620 °C (see Fig. 3). This phenomenon may be explained by assuming that iron sulphide, formed from pyrite, reacts with the water forming abundantly in coal decomposition according to the equation

$$3FeS + 4H_2O \rightleftharpoons Fe_3O_4 + 3H_2S + H_2 \qquad (1)$$

Levy and White [4] proved experimentally that this reaction starts at 560 °C. The first, broad peak of the H_2S curve coincides with the production of the aliphatic hydrocarbon products, indicating that a considerable amount of H_2S forms in the radical mechanism of the decomposition of the aliphatic side groups. The amount of H_2S formed in this region showed some

correlation with the organic sulphur content of the samples. COS, CS_2 and CH_3SH evidenced similar, but lower, double peaks. The second peaks of these intensities, however, were less strongly expressed than in the case of H_2S and may be due to secondary reactions between the H_2S formed by eqn. (1) and various coal decomposition products.

Kinetics of the overall mass loss of the sample

Because of the high precision of computer-aided TG measurements and the lower precision of our MS data, only the TG and DTG data were used for kinetic evaluation. We accepted the hypothesis stating that the thermal decomposition of coals can be approximated by an infinite number of parallel reactions with a general distribution of the activation energy [8]. We also accepted that the distribution of the activation energy can be approximated by a discrete set of parallel reactions [8]. We do not agree, however, with the opinion that all of these reactions can be described by the same pre-exponential factor. We do not believe that the partial reactions of coal decomposition are simple unimolecular processes. The low temperature decarboxylation and dehydration are probably the sums of forward and backward reactions while the decomposition of the alkyl side groups has a radical mechanism. In this way each partial reaction must have a separate formal kinetic approximation:

$$d\alpha_i/dt = A_i \exp(-E_i/RT) f_i(\alpha_i) \tag{2}$$

where α_i, A_i and E_i denote the reacted mole fraction, pre-exponential factor and activation energy respectively. If first-order kinetics is assumed for the partial processes, then

$$f_i(\alpha_i) = 1 - \alpha_i \tag{3}$$

The first-order hypothesis, however, is not really necessary; the calculations give approximately the same results for any $f_i(\alpha_i)$ functions. The number of partial processes is high; it can be regarded as infinite. Following Burnham et al. [8], we shall use only a discrete set of reactions as an approximation and will describe the overall reaction by

$$d\alpha/dt = \Sigma c_i \, d\alpha_i/dt \tag{4}$$

where α is the reacted fraction of the coal sample and c_i expresses the contribution of the ith partial reaction to the overall mass loss.

Coal sample S was used for the kinetic evaluation. Experiments were carried out at 5, 10, 20, 40 and 80 °C min^{-1}. As Fig. 4 shows, the corresponding DTG curves evidenced the usual shift to higher temperatures at higher heating rates but otherwise were very similar to each other. The similarity is well illustrated by the sample mass at the peak maximum: it was found to be 87.8% of the initial sample mass at all heating rates with a

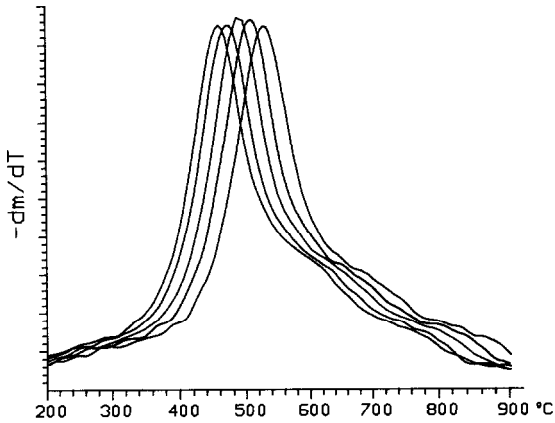

Fig. 4. DTG curves of coal S at five different heating rates. (For the correct scaling DTG is defined here as $-\mathrm{d}m/\mathrm{d}T$. The full scale of the figure is 0.13% $^{\circ}C^{-1}$.)

standard deviation of 0.08%. (This value corresponds to a reacted fraction $\alpha = 0.437$ with a standard deviation of 0.004). The good agreement in the shape of the DTG curves suggests that the points having identical reacted fractions at different heating rates correspond to an identical state of the decomposition. Hence we may assume that the peak maximum of a given partial reaction falls to (approximately) the same α value at 5 and 80 °C min^{-1}. In this way we can calculate the activation energies of the partial reactions by the dependence of the temperature of the corresponding points of the DTG curves on the heating rate. A simple and well-known approximation for this purpose is [12]

$$\ln\left(H/T_{\mathrm{peak}}^2\right) \approx \text{constant} - E_i/RT_{\mathrm{peak}} \tag{5}$$

where H is the heating rate and T_{peak} is the temperature of the highest reaction rate $\mathrm{d}\alpha_i/\mathrm{d}t$ of the given reaction. In the present age of computers, however, we do not really need linearisations of this type, since we can easily solve numerically the more correct least-squares minimisation of

$$S = \Sigma\left[\left(T_{\mathrm{peak}}\right)^{\mathrm{obs}} - \left(T_{\mathrm{peak}}\right)^{\mathrm{calc}}\right]_j^2 \tag{6}$$

where the subscript j indicates the jth heating rate and $(T_{\mathrm{peak}})^{\mathrm{obs}}$ and $(T_{\mathrm{peak}})^{\mathrm{calc}}$ denote the observed and the calculated values of T_{peak}. The equations used for the calculation of $(T_{\mathrm{peak}})^{\mathrm{calc}}$ with an arbitrary precision have been published previously [12,13]. In the case of a given $f_i(\alpha_i)$, $(T_{\mathrm{peak}})^{\mathrm{calc}}$ is a function of E_i and A_i. If $f_i(\alpha_i)$ is not known, $(T_{\mathrm{peak}})^{\mathrm{calc}}$ is a function of E_i and a formal constant. In the present work we assumed first-order kinetics to obtain A_i values also. The calculations were carried out at the DTG peak maximum and at discrete α_i values in the range [0.1, 0.95]. The results are shown in Table 2. The $(T_{\mathrm{peak}})^{\mathrm{obs}}$ values in the second and third columns of Table 2 are those experimental temperatures of the TG

TABLE 2

Results of the kinetic calculations

α	$(T_{peak})^{obs}$ (5 °C min^{-1}) (°C)	$(T_{peak})^{obs}$ (80 °C min^{-1}) (°C)	Deviation (°C)	Relative deviation (%)	$\log_{10} A$ (s^{-1})	E (kJ mol^{-1})
0.437	459	522	1.0	1.6	11.8	199
0.10	259	333	4.6	6.1	6.2	90
0.15	335	401	2.9	4.8	8.6	130
0.20	381	444	0.9	1.4	10.2	158
0.25	407	468	0.9	1.5	11.2	177
0.30	425	486	0.6	1.0	11.7	188
0.35	439	501	0.7	1.1	11.7	193
0.40	451	513	0.8	1.3	11.8	197
0.45	462	524	0.8	1.2	12.0	203
0.50	474	536	0.7	1.1	12.2	208
0.55	487	548	0.7	1.2	12.7	220
0.60	504	564	0.6	1.0	13.4	235
0.65	525	583	0.9	1.6	14.2	253
0.70	550	608	1.0	1.7	14.8	270
0.75	579	637	1.2	2.4	15.4	289
0.80	613	672	1.7	2.9	15.5	303
0.85	652	709	2.0	3.5	16.5	334
0.90	701	761	3.0	6.0	17.0	362
0.95	766	824	3.7	6.4	18.4	412

curves which belong to the given reacted fraction at the lowest and highest heating rates respectively. The first line contains the kinetic parameters calculated from the temperatures of the DTG peak maximum ($\alpha = 0.437$). The deviations in the fourth column of Table 2 were calculated by the formula S/N, where S is the least-squares sum (see eqn. (6)) and N is the number of observations. The deviations are lower than 1 °C from $\alpha = 0.2$ to $\alpha = 0.7$ and relatively higher at the flat beginning and end of the DTG curves. In the fifth column, under the heading "relative deviation", the deviations are divided by the differences between the highest and lowest experimental T_{peak} values at the same α. The relative deviations defined in this way are characteristic of the uncertainty of the obtained activation energies [13]. Until $\alpha = 0.6$ (below 530 °C at 5 °C min^{-1}) the E and A values are lower than the magnitudes corresponding to unimolecular reactions. This observation may be due to diffusion control (during dehydration and decarboxylation) and a radical mechanism (in the decomposition of the aliphatic structures). Note that chemical backward reactions can result in diffusion control at the applied heating rates [14]. From $\alpha = 0.65$ to $\alpha = 0.9$ the magnitudes of the A and E values fall in the magnitude range of unimolecular reactions, which may be interpreted in such a way that in this region the rupture of the chemical bonds is the rate-determining factor.

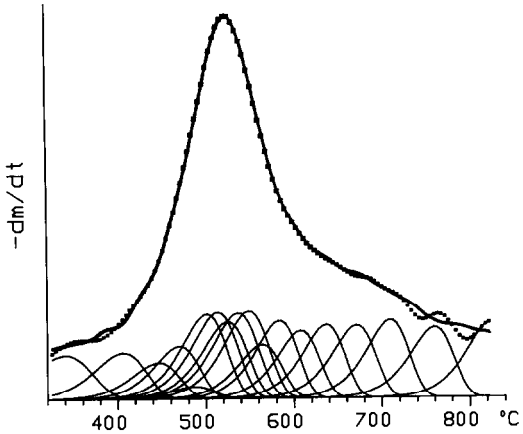

Fig. 5. DTG curve of coal S at 80 °C min^{-1} approximated by the sum of parallel reactions (see the text): ——, experimental curve; ■, sum of the partial reactions; ———, partial reactions.

Above $\alpha = 0.9$ the TG curve is too flat for this type of kinetic evaluation. It may be interesting to note that the weighted sum of these partial reactions (eqn. (4)) can describe the DTG curves with a good fit (see Fig. 5). The weight factors (c_i) were also calculated by the method of least squares.

CONCLUSIONS

The wide temperature domains and multiple peaks of the oxygen-containing products indicated the multiple sources of these compounds. A reaction of pyrite resulted in a second peak on the intensity curves of H_2S, COS, CS_2 and CH_3SH. The SO_2 production is connected with the pyrite content of the samples and seems to be the result of the oxidation of elemental sulphur or some other labile intermediate product with the oxygen traces of the inert ambient gas. The kinetic evaluation of the thermogravimetric curves at several heating rates showed that unimolecular reactions can be rate-determining factors only in the last third of the decomposition, between the evolution of about 60% and 90% of the volatile matter of the sample. Below this domain, relatively low pre-exponential factors and activation energies were observed owing to diffusion control at low conversions and a radical mechanism at medium conversions.

REFERENCES

1 P. Szabó, G. Várhegyi, F. Till and T. Székely, Thermochim. Acta, 170 (1990) 167.
2 A. Attar and G.G. Hendrickson, in R.A. Meyers (Ed.), Coal Structure, Academic Press, New York, 1982, p. 87.

3 W.H. Calkins, Energy Fuels, 1 (1987) 59.
4 J.H. Levy and T.J. White, Fuel, 67 (1988) 1336.
5 K. Chatterjee, B. Bal, L.M. Stock and R.F. Zabransky, Energy Fuels, 3 (1989) 427.
6 G.R. Gavalas, Coal Pyrolysis, Elsevier, Amsterdam, 1982.
7 M.A. Serio, D.G. Hamblen, J.R. Markham and P.R. Solomon, Energy Fuels, 1 (1987) 138.
8 A.K. Burnham, M.S. Oh, R.W. Crawford and A.M. Samoun, Energy Fuels, 3 (1989) 42.
9 H.N.S. Schafer, Fuel, 58 (1979) 667.
10 H.N.S. Schafer, Fuel, 58 (1979) 673.
11 M. Siskin and T. Aczel, Fuel, 62 (1983) 1321.
12 G. Várhegyi, Thermochim. Acta, 25 (1978) 201.
13 G. Várhegyi and T. Székely, Thermochim. Acta, 57 (1982) 13.
14 G. Pokol and G. Várhegyi, CRC Crit. Rev. Anal. Chem., 19 (1988) 65.